Hindawi
Science and Technology of Nuclear Installations
Volume 2020, Article ID 8819794, 13 pages
https://doi.org/10.1155/2020/8819794

Research Article

Monte Carlo Simulation and Experimental Validation for Radiation Protection with Multiple Complex Source Terms and Deep Penetration for a Radioactive Liquid Waste Cementation Facility

Wenqian Li,[1] **Xuegang Liu**,[1] **Sheng Fang**,[1] **Xueliang Fu**,[2] **and Kaiqiang Guo**[2]

[1]*Institute of Nuclear and New Energy Technology, Collaborative Innovation Centre of Advanced Nuclear Energy Technology, Key Laboratory of Advanced Reactor Engineering and Safety, Ministry of Education, Tsinghua University, Beijing 100084, China*
[2]*CNNC Everclean Environmental Engineering Co., Ltd., Beijing 100037, China*

Correspondence should be addressed to Sheng Fang; fangsheng@tsinghua.edu.cn

Received 8 June 2020; Revised 14 September 2020; Accepted 24 September 2020; Published 8 October 2020

Academic Editor: Peter Ivanov

A new radioactive liquid waste cementation facility was under commissioning recently in the Institute of Nuclear and New Energy Technology of Tsinghua University, which is designed to simultaneously process multiple intermediate-level radioactive waste drums. Therefore, the multiple volume sources and the scattering effect becomes a key issue in its radiation protection. For this purpose, the Monte Carlo program FLUKA code and experimental measurement were both adopted. In the FLUKA simulation, five different scenarios were considered, i.e., one drum, two drums, four drums, six drums, and eight drums. For the multiple volume sources, the source subroutine code of FLUKA was rewritten to realize the sampling. The complex shielding also leads to a deep penetration problem; hence, the optimization algorithm and variance reduction techniques were adopted. During the measurement, two scenarios, outdoor and indoor, were carried out separately representing the dose field when only one drum is considered and when the scattering effect is considered. A comparison between the experiments and calculations shows very good agreement. From both of the Monte Carlo simulation and the experimental measurement, it can be drawn that, in the horizontal direction, with the increase of the drum number, the dose rate increases very little, while in the vertical direction, the increase of the dose rate is very obvious with the increase of the drum number. The complicated source term sampling methods, the optimization algorithm and variance reduction techniques, and the experimental verification can provide valuable references for the similar scattering problem in radiation protection and shielding design.

1. Introduction

For a room with walls, roof, and other structures, when considering the dose from a gamma radiation source to the point of interest, if the scattering effect is ignored, the dose may be underestimated. In addition, when several radioactive sources exist, the total dose contribution of these radioactive sources to the point of interest should be considered. However, it will be extremely difficult to accurately predict the dose distribution when each gamma source is covered with multiple shielding layers so that the dose outside the shielding is very low.

In this work, the radiation protection of a radioactive liquid waste cementation facility is investigated, which meets the above scenario. This facility is located at the Institute of Nuclear and New Energy Technology (INET) [1] of Tsinghua University, China. The facility is a room for processing radioactive waste storage drums, with a sliding track and an iron shielding, as shown in Figure 1. In actual operation, there may be multiple intermediate-level radioactive waste (ILW) drums in the room. Every drum contains about 2E10 Bq of Cs-137, and the surface dose rate for one drum may exceed 3 mSv/h [2]. These drums will be placed on the sliding track. Although there is an iron shielding of 12 cm

(a) (b) (c)

Figure 1: Photos for the radioactive liquid waste cementation facility shows (a) the roof, the walls, and the shielding, (b) the sliding track, and (c) the intermediate radioactive waste storage drum when it was uncovered.

thickness which can be remotely controlled to move up and down, from Figure 1(a), it can be seen that when multiple drums exist behind the shielding, the photons reflected by the roof to the front of the shielding may greatly increase the dose in the operation area. For the safety of the staff, an accurate assessment of the dose field from the multiple complex source term will be very necessary.

However, each ILW drums contains multiple shielding layers, as shown in Figure 1(c), which is to ensure the dose rate on the drum surface meets the requirements of national regulations [3–6]. However, this kind of design also brings a deep penetration problem in the Monte Carlo simulation [7–9], that is, when the shielding layers are too thick or the shielding structures are very complicated, if the number of simulated particles is low, the statistical result will be zero or obviously lower than the true value. Only when the number of simulated particles is large enough, the accurate result can be obtained. So, when multiple ILW drums coexist, this deep penetration problem will be very apparent.

The purpose of this work is to research the accurate calculation method of the dose field distribution under this kind of multiple source term and deep penetration condition. Traditional theoretical formula prediction methods, such as the QAD program [10–13] which is based on point-kernel integration technology [14–16], can quickly perform the shielding calculation, but usually, the calculation results are too conservative. Currently, there are many Monte Carlo programs widely used, such as MCNP [17–19], FLUKA (http://www.fluka.org/fluka.php) [20], and GEANT4 [21, 22], which have been verified, can provide very accurate simulation results [23].

For the multiple-source term problem, whether adopting the empirical formula method or the Monte Carlo method, the dose field distribution corresponding to each source can be calculated one by one then summed. However, this method is time consuming for successive data processing. This work attempts to adopt the FLUKA program and rewrite the source subroutine code to realize the sampling of multiple volume sources in one calculation routine and give the total dose field results, which greatly reduces the workload for the data processing.

For the deep penetration problem, different variance reduction techniques can be adopted. Based on the previous work [2], this work comprehensively considers the room walls, roof, internal structures, and all drums. Then, the optimization algorithm and variance reduction techniques proposed in [2] were adopted to complete the simulation calculation.

Furthermore, to verify the accuracy of the above method, an experiment was carried out and the measurement results were compared with the calculation result. The experiment was carried out under two scenarios: one is the outdoor measurement, which represents the dose field when only one drum is considered; another is the indoor measurement, which represents the dose field when the scattering effect is considered. In this way, the accuracy of the Monte Carlo calculation is verified by the actual measurement.

The complicated source term sampling methods, the optimization algorithm and variance reduction techniques, and the experimental verification can provide valuable references for similar problems in radiation protection and shielding design.

2. Materials and Methods

2.1. Monte Carlo Simulation

2.1.1. Geometry Models and Material

(1) The ILW Drum. The detailed description of the geometry structure and materials compositions for one ILW drum can be found in previous work [2]. From outside to inside, one ILW drum consists of the following four parts: (1) the standard 200L steel drum, (2) the cement inner shielding layer, (3) the auxiliary support structure, and (4) the cement solidified radioactive waste. The standard 200L steel drum is 56 cm in diameter and 85 cm in height. The cement inner shielding layer is 6 cm of thickness. The auxiliary support

structure is specially designed with stainless steel of 1.0 mm thickness. The radioactive waste in the solidified cement form was filled in the inside. Figure 2 shows the geometry model of one ILW storage drum.

(2) Room and Shielding Structure. In the real operating environment, multiple ILW storage drums will be placed in the room. Figure 3 shows the geometry model of the room and shielding structures. The room is 11 m of length, 2.6 m of width, and 3.5 m of height. Walls are made of ordinary concrete with 50 cm of thickness. The drums will be transported on an iron sliding track with 8 m of length, 0.8 m of width, and 17 cm of thickness. An iron shielding with 12 cm of thickness and 1.5 m of height is set to separate the high dose area and the operating area. In the calculation model, it was assumed that the center axis distance of two adjacent drums is 82 cm. The sliding track can hold up to eight ILW storage drums.

2.1.2. Source Term. The radioactive source is homogeneously distributed in the solidified cement (i.e., part 4 in Figure 2). As described in the previous work [2], the radioactive waste is from the spent nuclear fuel reprocessing process, and dominant includes Cs-137 and Sr-90 (>95% of the total activity). In the simulation calculation, only Cs-137 was taken into account. And only the gamma ray of the highest energy (661.6 keV with a branching ratio of 85.1%) was considered, while the gamma rays of lower energies were ignored.

Different from previous work [2], the actual total activity of Cs-137 was detected in this work. The measured gamma intensity was 2.05E10 γ/s, which is 0.87-fold of the designed highest total activity.

Based on the above, the source shape should be a cylinder that exists inside each ILW drum. When multiple drums exist simultaneously, there are multiple volume sources. In this work, the "source.f" source file in the FLUKA program was rewritten to achieve the Monte Carlo sampling of multiple volume sources. The detailed method is as follows.

First, sample the drum that the volume source should belong to. Assuming there are m numbers of drums. Figure 4 shows the flowchart to sample which drum the source particle comes from, where rand_n represents the nth random number.

Then, sample the source particle position *(x, y, z)* by Eqs. (1)–(4):

$$r = R \times \max\left(\text{rand}_2, \text{rand}_3\right), \tag{1}$$

$$x = r \times \sin\left(\text{rand}_4\right) + d_m, \tag{2}$$

$$y = r \times \cos\left(\text{rand}_4\right), \tag{3}$$

$$z = h_1 + h_2 * \text{rand}_5, \tag{4}$$

where R is the radius of the cylinder; d_m is the horizontal distance from the central axis of the drum to the origin of the

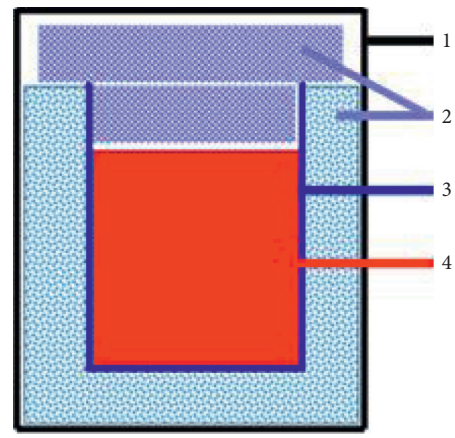

1. The standard 200L steel drum
2. The cement inner shielding layer
3. The auxiliary support structure
4. The cement solidified radioactive waste

Figure 2: Geometry model of an ILW storage drum.

x-axis; and h_1 and h_2 are the height coordinates of the bottom and top surfaces of the cylinder respectively. Eqs. (1)–(4) realize homogeneous sampling in a cylinder.

Third, sample the emission direction *(u, v, w)* of the source particles by equations (5)–(9):

$$w = \cos\theta = 1 - 2 \times \text{rand}_6, \tag{5}$$

$$\sin\theta = \sqrt{1 - \cos^2\theta}, \tag{6}$$

$$\varphi = \text{rand}_7 \times 2\pi, \tag{7}$$

$$u = \sin\theta \times \varphi, \tag{8}$$

$$v = \sin\theta \times \sin\varphi. \tag{9}$$

Eqs. (5)–(9) realize isotropic sampling.

Finally, it should be noted that the calculated result should be multiplied by a normalization factor that takes the number of drums into account to obtain the final dose matrix.

2.1.3. Cutoff Energy and Variance Reduction Technique. The cutoff energy is under the assumption that if the transported particle cannot go out from the current layer with enough energy, its contribution to the final statistical result is negligible. So, if the particle energy is lower than the cutoff energy, the particle will be killed. The variance reduction technique adopted in this work is based on the Russian Splitting skill: if a transported particle goes into the region with splitting number N, the particle will split into N particles and every split particle will weight $1/N$. In the previous work [2], it has been verified that proper cutoff energy and variance reduction technique settings can improve the calculation efficiency more than 20 times, while the deviation of the calculation results is ignorable.

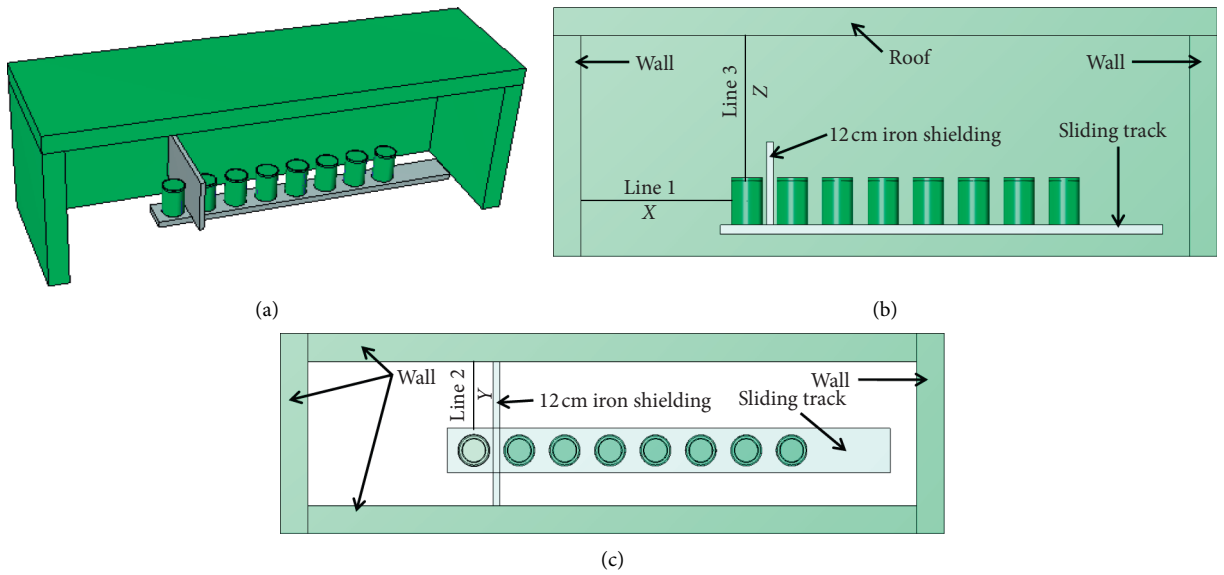

Figure 3: Geometry model of the room and shielding structures: (a) three-dimensional view, (b) front view, and (c) top view.

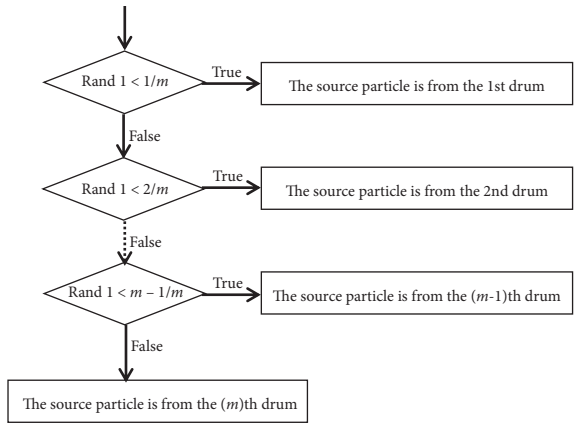

Figure 4: Flowchart to sample which drum the source particle comes from.

Therefore, in the Monte Carlo simulation of this work, the cutoff energy setting and variance reduction technique similarly as in previous work [2] were also adopted. For the new geometry structures, including the surrounding walls, the roof, the sliding track, and the iron shielding, to reduce the influence on the accuracy of the calculation result, the cutoff energies were set very low and no variance reduction technique was set. The cutoff energy and variance reduction technique settings are summarized in Table 1.

2.1.4. Dose and Error. In the FLUKA simulation, the ambient dose equivalent, H∗(10), were scored for five scenarios: one drum, two drums, four drums, six drums, and eight drums. The conversion coefficients are taken from the ICRP Publication 74 [24, 25]. The FLUKA program provides the three-dimensional dose matrix. The software SimpleGEO (http://www.fluka.org/fluka.php) can read and process the dose matrix and give a 3D display.

Three interesting lines are drawn out in Figures 3(b) and 3(c). Line 1 and line 2 are along the X-axis and Y-axis, respectively, representing the distance to the side surface of the first drum. Line 3 is along the Z-axis, representing the distance to the top of the first drum. Dose comparisons along these three lines were made to evaluate the scattering effects and dose distribution in the operating area.

Corresponding with the three-dimensional dose matrix results in the FLUKA calculation, an error matrix will be given. By increasing the number of simulated particles, the statistical errors can be reduced. Also, it can be seen from the 3D dose display figure that smoother the color transition, the smaller the error. In this work, the error is controlled less than 3% by adopting enough transported particle number and parallel calculation. The total numbers of transport particles were more than $2e9$.

However, the use of the variance reduction method may bring other errors. In this regard, the experimental measurement method was adopted for comparison, which shows that the simulation calculation results are in good agreement with the measurement results (see Section 3.3). So, it can be believed that the error caused by the variance reduction method is negligible.

2.2. Experimental Measurement

2.2.1. Measurement Equipment. The measurement equipment is the ambient dose rate meter (9DP), as shown in Figure 5. In addition, the measurement props also include a lead apron, two rulers, and a telemeter rod.

2.2.2. Measurement Scenarios. During measurement, two scenarios, outdoor and indoor, were adopted, representing the cases without and with scattering considered, respectively.

Table 1: The cutoff energy and variance reduction technique settings.

Regions	Cutoff energy of electron and photon (keV)	Splitting number
(1) The standard 200L steel drum	1	4
(2) The cement inner shielding layer	9	2
(3) The auxiliary support structure	9	2
(4) The cement solidified radioactive waste	80	—
(5) The sliding track	100	—
(6) The surrounding walls and the roof	90	—
(7) The iron shielding	90	—

Figure 5: Photos of the ambient dose rate meter (9DP).

(1) Scenario 1 (outdoor). The outdoor measurement can reflect the dose field distributions with no affection by scattering.

Before measurement, a ruler was fixed vertically to the outside of the drum, and another ruler was placed horizontally on the ground along the symmetry axis of the drum, as shown in Figure 6(a). Then, the surveyor held a telemeter rod and the monitor and measured along the horizontal ruler, as shown in Figure 6(b). The horizontal measured positions include 1/2/3/4/5 meters to the outside of the drum. The vertical measurement only includes a height of 50 cm above the ground.

(2) Scenario 2 (indoor). The indoor measurement can reflect the dose field distributions under the scattering effect. During measurement, eight drums were all put on the sliding track, in which, seven drums were behind the iron shielding, and one was out of the shielding. Figure 7 was taken during the measurement. The horizontal measured positions include 10 cm/50 cm/1 m/2 m to the outside of the drum. The vertically measured position was at the half-height of the drum.

2.2.3. Uncertainty Estimation of Measurement. The statistical uncertainties (Type A) and the systematic uncertainties (Type B) were considered for the experimental error.

The statistical uncertainty can be calculated by

$$U_A = \frac{\sqrt{(1/N-1)\sum_{i=1}^{N}\left(X_i - \overline{X}\right)^2}}{\sqrt{N}}, \tag{10}$$

where U_A is the statistical uncertainty of the samples, $\overline{X}$ is the mean value of the replicate measurement, and N is the number of the replicate measurements, which is in the range of 5 to 10.

The systematic uncertainty can be calculated by

$$U_B = \frac{\sqrt{\Delta_i^2 + \Delta_e^2}}{\sqrt{3}} = \frac{\overline{X}\sqrt{E^2 + V^2}}{\sqrt{3}}, \tag{11}$$

where U_B is the systematic uncertainty, Δ_i is the instrument error, Δ_e is the estimation error which comes from the measurement object, environment, and human factors, etc., and E and V are the relative inherent error and the measurement standard deviation, respectively. According to the equipment verification certificate, $E = 11.4\%$ and $V = 2.3\%$.

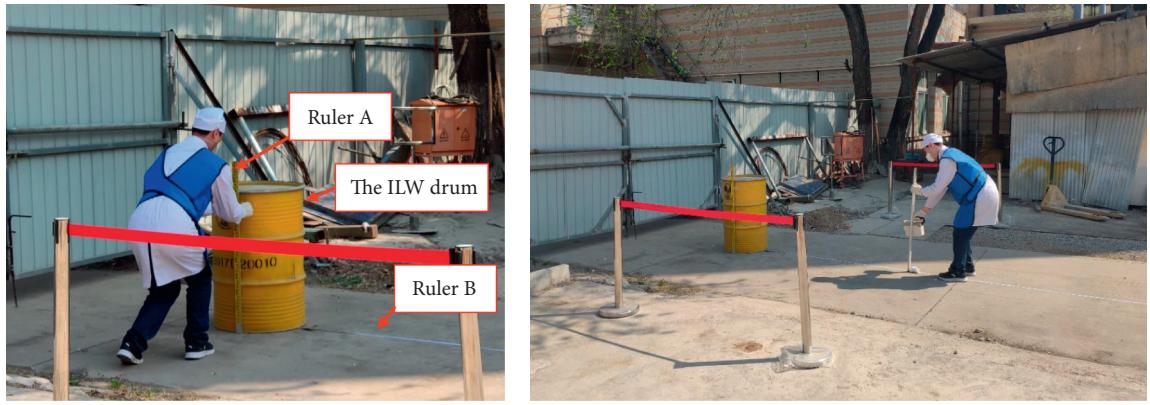

(a) (b)

Figure 6: Photos during the outdoor measurement.

Figure 7: Photos during the indoor measurement.

Then, the combined uncertainty of measurement (U) can be calculated by

$$U = \sqrt{U_A^2 + U_B^2}. \quad (12)$$

3. Results and Discussion

3.1. FLUKA Simulation Results. In the previous work [2], only the dose distribution within 15 cm from the drum surface was calculated. This work mainly focuses on the real dose field distribution when there are several drums in the room, and the scattering effect from other structures such as the walls should also be concerned. The size of the dose field considered is 11 m of length, 2.6 m of width, and 3.5 m of height.

3.1.1. 3D Dose Rate Distribution. Figure 8 gives the results of three-dimensional dose distribution for the five scenarios: one drum, two drums, four drums, six drums, and eight drums. For each scenario, the 3D view shows the three plans intersect at the center point of the first drum. Then, the front view and the top view, respectively, correspond to the section position in the 3D view.

For the scenario of one drum, the FLUKA simulated results indicate that the dose rates on the other side of the iron shielding are rather low, generally lower than 10 μSv/h. As the number of drums increases, the dose rates also increased significantly on the other side of the iron shielding. And the dose rates directly above the drums are usually higher. When there are eight drums on the sliding track, the dose rates on the inside (right side in the front view) of the iron shielding generally range from 76 μSv/h to 5 mSv/h, and this area will be forbidden entrance during operation.

3.1.2. Dose Rate Distribution along the Three Lines of Interest. It was observed that, with the increase of the drum number, the dose rates outside iron shielding would also increase. Since the iron shielding is designed to be liftable and the area above iron shielding is unshielded, the gamma rays may enter the work area by scattering of the walls and roofs. This kind of physical mechanism was not considered in the previous design for one drum. To compare the effect of scattering on the dose rate in the working area, the dose rates on the three lines of interest shown in Figures 3(b) and 3(c) were extracted from the three-dimensional dose matrix and plotted in Figure 9.

It can be seen from Figures 9(a) and 9(b) that, in the horizontal direction (Line 1 and Line 2), with the increase of the drum number, the dose rate increases very little. In line1, at a position of 2.5 m from the first drum surface was quite near the wall, the dose rate is 79 ± 2 μSv/h for one drum scenario, while the dose rate is 84 ± 3 μSv/h for eight drums scenario. Similarly, in line 2, at a position of 1.1 m from the first drum surface, the corresponding dose rates are 269 ± 8 and 274 ± 8 μSv/h for one drum and eight drums' scenario, respectively.

It can be seen from Figure 9(c) that, in the vertical direction (Line 3), the increase of the dose rate is very obvious with the increase of the drum number. In the case of one drum and eight drums, at 1 m from the top surface of the first drum, the corresponding dose rates are 112 ± 3 and 195 ± 6 μSv/h, respectively. And at 1.5 m, the two values were 62 ± 2 and 177 ± 5 μSv/h, which increased by nearly three times. At 2.5 m, the two values were 31 ± 1 and 140 ± 4 μSv/h, which increased more than four times.

In summary, in the horizontal direction corresponding to the middle of the drum, the increase of the dose rate is not obvious, while in the vertical direction, the dose rate increase by scattering is significant and unneglectable.

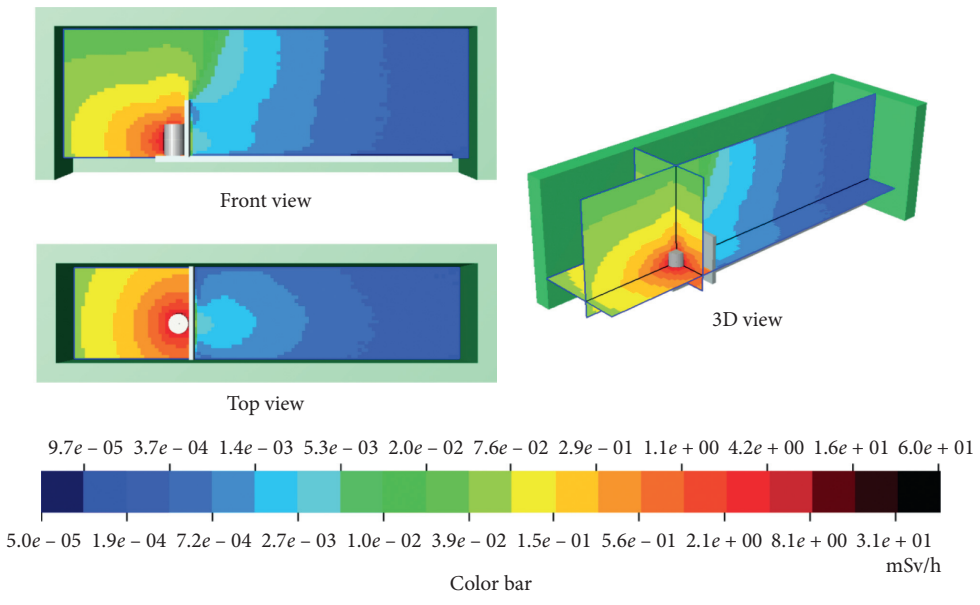

(a)

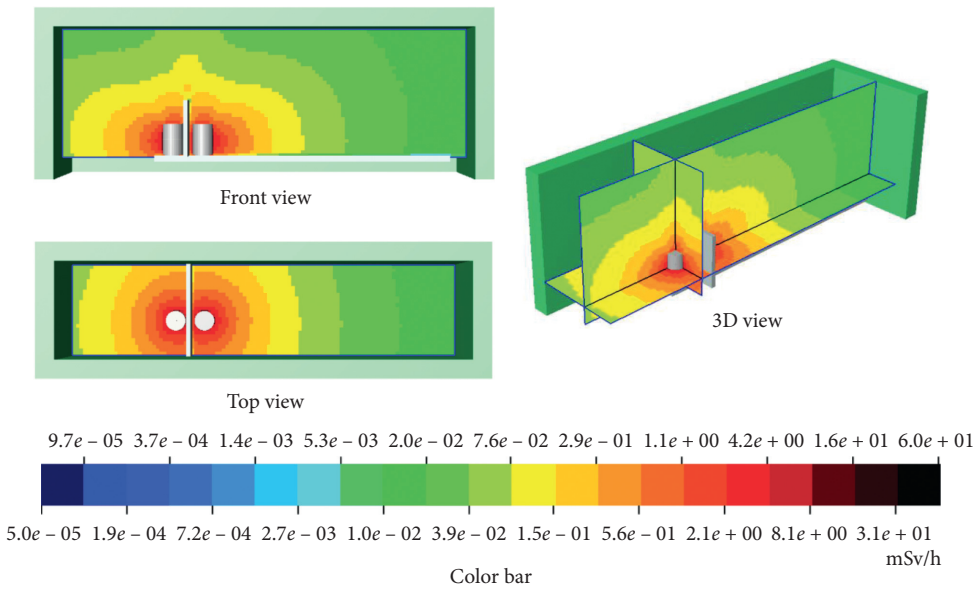

(b)

Figure 8: Continued.

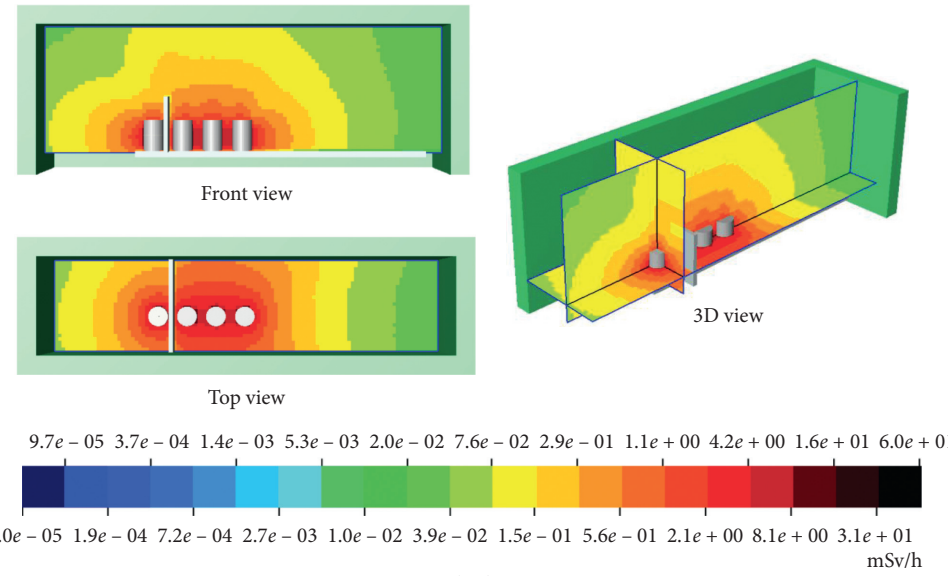

(c)

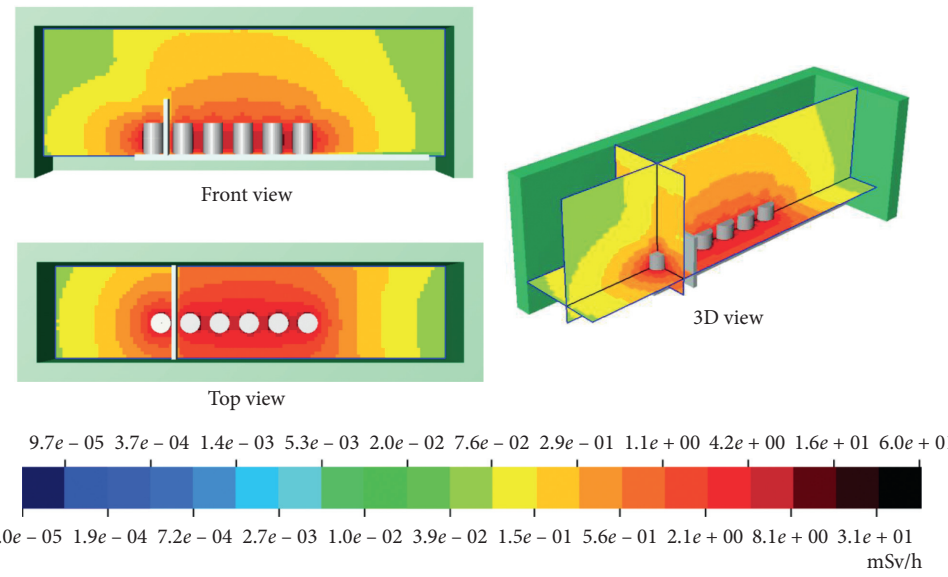

(d)

Figure 8: Continued.

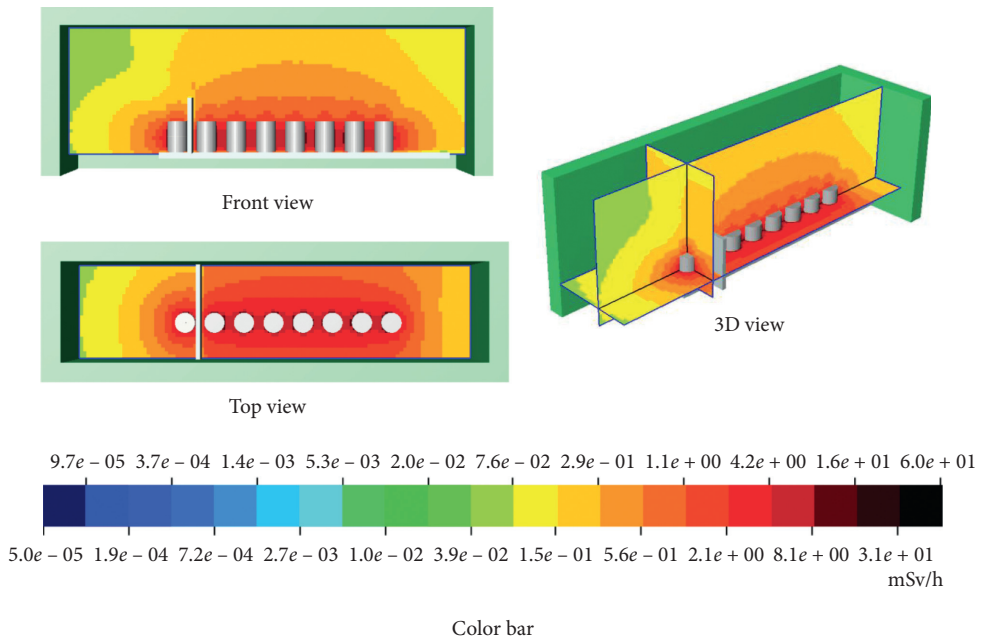

(e)

Figure 8: The front views, the top views, and the 3D views for the five scenarios: one drum, two drums, four drums, six drums, and eight drums.

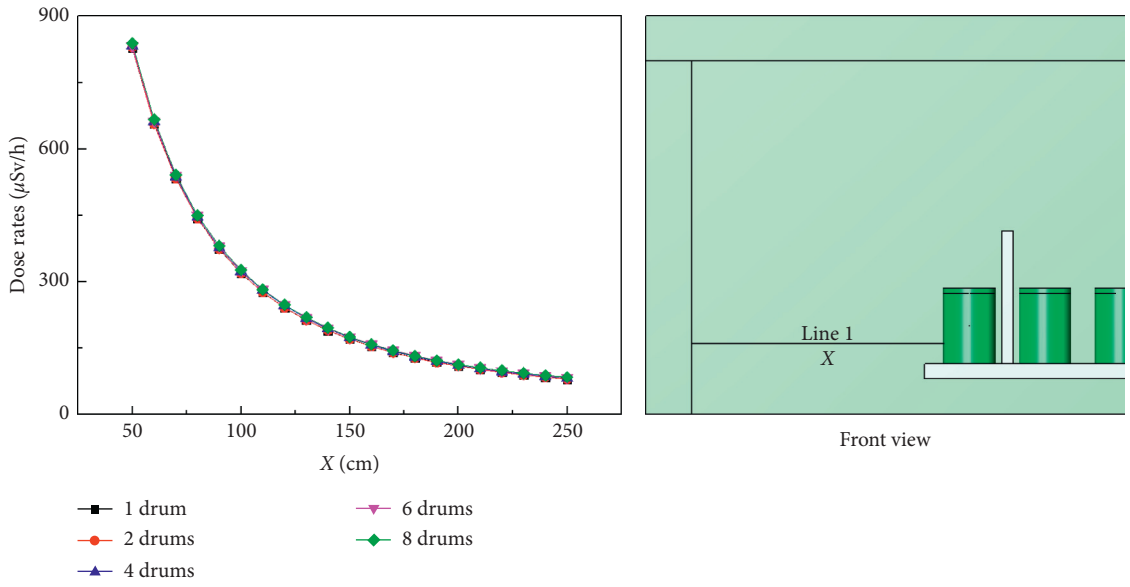

(a)

Figure 9: Continued.

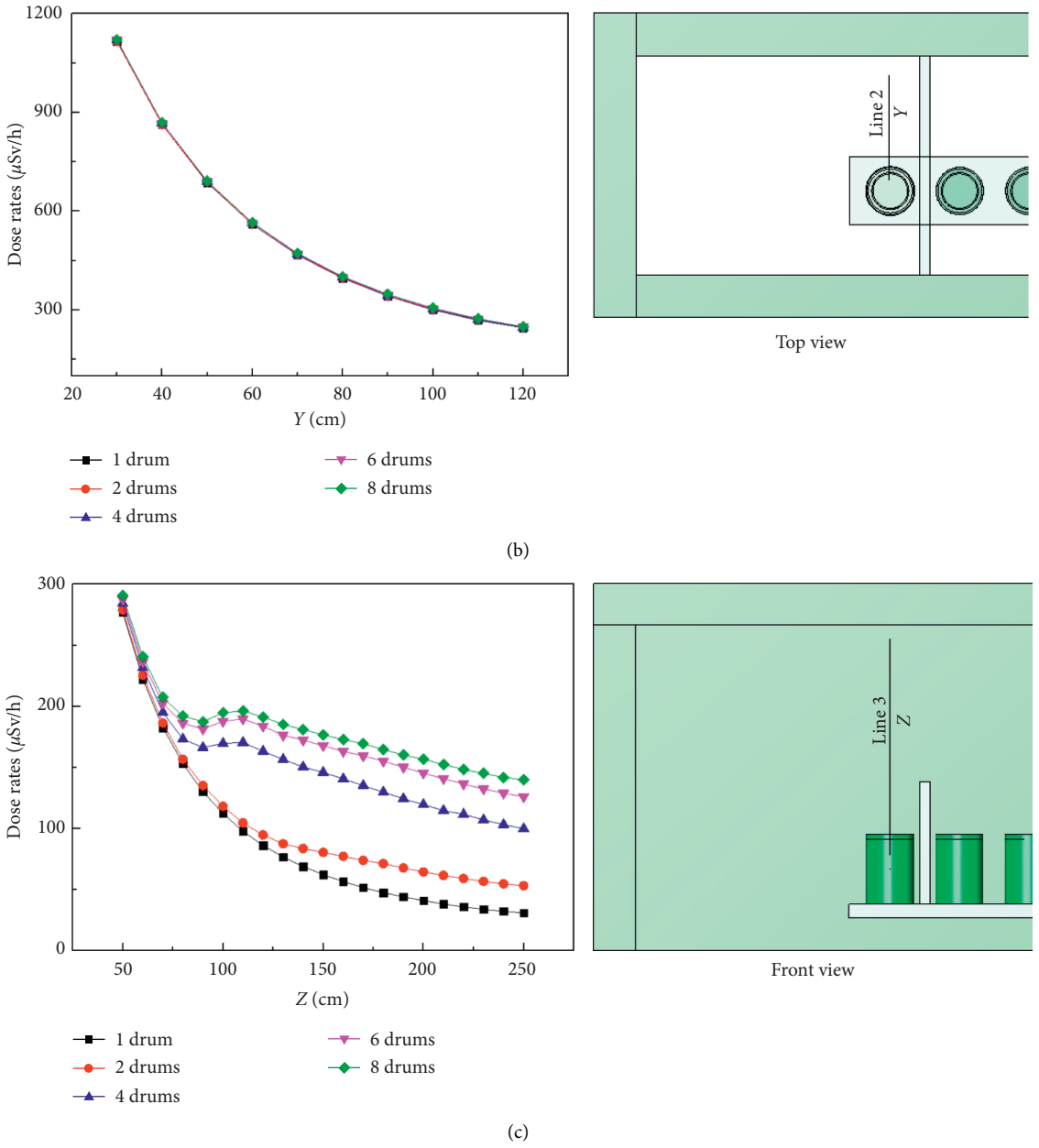

Figure 9: The dose rate distribution along the three lines of interest for the five scenarios. (a) Line 1. (b) Line 2. (c) Line 3.

3.2. Experimental Measurement Results

3.2.1. Measurement Results for Outdoor. Table 2 lists the outdoor measured ambient dose equivalent results which can reflect the dose field distributions with no affection by scattering. The horizontal measured positions include 1/2/3/4/5 meters to the outside of the drum. The vertical measurement was at a height of 50 cm above the ground. The corresponding FLUKA simulation results are also listed in Table 2. From the ratio of the FLUKA calculated and measured $H*(10)$ (F/M value), which ranges from 1.4 to 1.5, it can be seen that the differences between the measurement and the FLUKA simulation are within two times.

3.2.2. Measurement Results for Indoor. Table 3 lists the indoor measured ambient dose equivalent results which can reflect the dose field distributions affected by scattering. In this scenario, seven drums were behind the iron shielding on the sliding track, and one was out of the shielding. The horizontal measured positions include

Table 2: The outdoor measured $H*(10)$ compared with the FLUKA calculated results.

Distance to the drum	$H*(10)$/uSv/h		F/M value
	Measurement value	FLUKA calculation	
1	170 ± 10	251 ± 8	1.5
2	60 ± 4	85 ± 3	1.4
3	29 ± 2	42 ± 1	1.4
4	17 ± 1	24.5 ± 0.7	1.4
5	11.3 ± 0.8	16.2 ± 0.5	1.4

Table 3: The indoor measured $H*(10)$ compared with the FLUKA calculated results.

Distance to the drum (m)	$H*(10)/\mu$Sv/h		F/M value
	Measurement value	FLUKA calculation	
10	1190 ± 80	3120 ± 90	2.6
50	410 ± 30	840 ± 30	2.0
1	180 ± 10	330 ± 10	1.8
2	58 ± 4	113 ± 3	1.9

10 cm/50 cm/1 m/2 m to the outside of the drum. The vertically measured position was at the half-height of the drum. The corresponding FLUKA simulation results are also listed in Table 3. From the F/M value, it can be seen that the FLUKA simulation results are about 1.8 to 2.6 times higher than the measurement results.

3.3. Comparison and Discussion. This work mainly focuses on the effect of scattering when there are several ILW drums in the operation room. From the above data and analysis, it can be seen that the calculated and measured results are in good agreement. Therefore, although the experimental data is relatively limited, it can be believed that the FLUKA simulation calculation can give very accurate results.

From the measurement results, at a distance of 1 meter from the drum, the $H*(10)$ for outdoor and indoor are $170 \pm 10\,\mu$Sv/h and $180 \pm 10\,\mu$Sv/h, respectively. And at a distance of 2 meters, outdoor and indoor results are $60 \pm 4\,\mu$Sv/h and $58 \pm 4\,\mu$Sv/h, respectively. These results show that, in the horizontal direction corresponding to the middle of the drum, the effect of scattering is not obvious, which is also consistent with the FLUKA calculated results.

From the FLUKA simulation results, which is also discussed in detail in Section 3.1, it is pointed out that, at a distance of more than 1 m from the top surface of the drum, as the height increases, the dose rate increases by scattering is significant.

4. Conclusions

In this work, the Monte Carlo program FLUKA was adopted to calculate the dose field distribution in a radioactive liquid waste cementation facility. The main emphasis was put on the effect of scattering when several ILW drums exist in the room. And measurement was made to verify the accuracy of the simulation calculation.

In the FLUKA simulation, by rewriting the source file, complex source sampling is realized when several ILW drums coexist. And the optimization algorithm and variance reduction techniques are adopted to improve the calculation efficiency. The above method can greatly reduce the time cost of calculation and results processing. The simulation was performed for the five scenarios: one drum, two drums, four drums, six drums, and eight drums exist. For each scenario, the three-dimensional dose field distribution was calculated and the corresponding 3D view, front view, and top view were given. The dose rate distributions along the three lines of interest were also analyzed.

The FLUKA simulation shows that, in the horizontal direction, with the increase of the drum number, the dose rate increases very little. Typically, at a position of 2.5 m away from the outside drum, the dose rate is $79 \pm 2\,\mu$Sv/h for one drum scenario and $84 \pm 3\,\mu$Sv/h for eight drums' scenario. While in the vertical direction, the increase of the dose rate is very obvious with the increase of the drum number. Typically, at 1.5 m from the top surface of the outside drum, the dose rates are 62 ± 2 and $177 \pm 5\,\mu$Sv/h for one drum's and eight drums' scenario, which increased by nearly three times. At 2.5 m, the two values were 31 ± 1 and $140 \pm 4\,\mu$Sv/h, which increased more than four times.

The measurement was performed for the two scenarios, outdoor and indoor, representing the cases without and with scattering considered, respectively. From the measurement results, at a distance of 1 meter from the drum, the $H*(10)$ for outdoor and indoor are $170 \pm 10\,\mu$Sv/h and $180 \pm 10\,\mu$Sv/h, respectively. A comparison between the experiments and calculations shows very good agreement. For the outdoor scenarios, the differences between the measurement and the FLUKA simulation are within two times. And for the indoor scenarios, the FLUKA simulation results are about 1.8 to 2.6 times higher than the measurement results. Therefore, although the experimental data is limited, the FLUKA calculation results for the whole dose field are accurate enough.

The complicated source term sampling methods, the optimization algorithm and variance reduction techniques, and the experimental verification can provide valuable references for the scattering problem in radiation protection and shielding design.

Abbreviations

ILW: Intermediate-level radioactive waste.

Data Availability

The data used to support the findings of this study are available from the corresponding author upon request.

Conflicts of Interest

The authors declare that they have no conflicts of interest.

Authors' Contributions

Data curation, formal analysis, software calculation, and writing of the original draft were carried out by Wenqian Li. Experiment supervision, data analysis, and funding acquisition were carried out by Xuegang Liu. Conceptualization, methodology, supervision, writing—review and editing—and funding acquisition were carried out by Sheng Fang. Experiment execution was carried out by Xueliang FU and Kaiqiang GUO.

Acknowledgments

This work was supported by the National Natural Science Foundations of China (Grant nos. 11875037 and 11475100) and foundation of Key Laboratory of Advanced Reactor Engineering and Safety, Ministry of Education (Grant no. ARES-2018-08). This work was partially supported by the Nuclear Facility Decommissioning and Radioactive Waste Treatment Foundation of China Atomic Energy Authority (Project no. 20134602025).

References

[1] S. Jiang, J. Tu, X. Yang, and N. Gui, "A review of pebble flow study for pebble bed high temperature gas-cooled reactor," *Experimental and Computational Multiphase Flow*, vol. 1, no. 3, pp. 159–176, 2019.

[2] W. Li, X. Liu, L. Ming et al., "Multilayer shielding design for intermediate radioactive waste storage drums: a comparative study between fluka and QAD-CGA," *Science and Technology of Nuclear Installations*, vol. 2019, Article ID 8186798, 2019.

[3] GB11806, *Radioactive Material Safe Transport Regulations*, Chinese National Standards Ministry of Ecology and Environment of the People's Republic of China , Beijing, China, 2004.

[4] GB14500, *Radioactive Waste Management Regulations*, Chinese National Standards Ministry of Ecology and Environment of the People's Republic of China, Beijing, China, 2002.

[5] F. G. Liu, L. P. Liu, F. F. Dong et al., *Discussion on the Minimization of Radioactive Waste of the Nuclear Power Plants in China*, Nuclear Standard Measurement and Quality Institute of Nuclear Industry Standardization of the People's Republic of China, China, Chinese, 2018.

[6] W. T. Zheng and X. J. Cheng, "Research on related problems of low and intermediate level radioactive waste disposal in China," *Energy Construction (Chinese)*, vol. 1, no. 1, pp. 75–82, 2014.

[7] Q. Pan and K. Wang, "An adaptive variance reduction algorithm based on RMC code for solving deep penetration problems," *Annals of Nuclear Energy*, vol. 128, pp. 171–180, 2019.

[8] Z. Zheng, Q. Mei, and L. Deng, "Study on variance reduction technique based on adjoint discrete ordinate method," *Annals of Nuclear Energy*, vol. 112, pp. 374–382, 2018.

[9] T. Shi, J. Ma, H. Huang et al., "A new local variance reduction method based on anti-forward Monte Carlo calculation," *Annals of Nuclear Energy*, vol. 115, pp. 595–600, 2018.

[10] R. E. Malenfant, *QAD: A Series of Point-Kernel General Purpose Shielding Programs*, Los Alamos Scientific Lab., Los Alamos, NM, USA, 1966.

[11] J. K. Shultis and R. E. Faw, "Radiation shielding technology," *Health Physics*, vol. 88, no. 4, pp. 297–322, 2005.

[12] W. Y. Wang, L. G. Zhang, J. Z. Cao et al., "Optimization of the radiation shielding program QAD," in *Proceedings of the 24th International Conference on Nuclear Engineering*, Charlotte, NC, USA, June 2016.

[13] W. Li, S. Fang, and H. Li, "Research on the induced radioactivity of HTR-PM's reactor pressure vessel: a comparative study between FLUKA, KORIGEN and QAD-CGA," *Annals of Nuclear Energy*, vol. 114, pp. 129–135, 2018.

[14] Y. Harima, "An historical review and current status of buildup factor calculations and applications," *Radiation Physics and Chemistry*, vol. 41, no. 4-5, pp. 631–672, 1993.

[15] I. M. Prokhorets, I. S. Prokhorets, S. Khazhmuradov et al., "Point-Kernel method for radiation fields simulation," *Problems of Atomic Science and Technology*, vol. 48, 2007.

[16] V. P. Singh and N. M. Badiger, "Comprehensive study of energy absorption and exposure build-up factors for concrete shielding in photon energy range 0.015–15 MeV up to 40 mfp penetration depth: dependency of density, chemical elements, photon energy," *International Journal of Nuclear Energy Science and Technology*, vol. 1, no. 7, pp. 75–99, 2012.

[17] B. Leal-Acevedo and I. Gamboa-deBuen, "Dose distribution calculation with MCNP code in a research irradiator," *Radiation Physics and Chemistry*, vol. 167, Article ID 108320, 2020.

[18] S. Shalbi, N. Sazali, and W. N. W. Salleh, "A simulation on desired neutron flux for the boron neutron capture therapy (BNCT) purpose by using Monte Carlo N-Particle (MCNPX)," *IOP Conference Series: Materials Science and Engineering*, vol. 736, Article ID 062022, 2020.

[19] D. B. Pelowitz, *MCNPX User's Manual*, Los Alamos National Laboratory Report, Los Alamos, NM, USA, 2008.

[20] A. Ferrari, P. R. Sala, A. Fasso et al., *FLUKA: A Multi-Particle Transport Code*, CERN European Organization for Nuclear Research, Geneva, Switzerland, 2008.

[21] Z. M. Hu, Y. H. Zheng, T. S. Fan et al., "Experimental evaluation of the Geant4-calculated response functions of a Bonner sphere spectrometer on monoenergetic neutron sources," *Nuclear Instruments & Methods in Physics Research Section A-Accelerators Spectrometers Detectors and Associated Equipment*, vol. 965, p. 6, 2020.

[22] S. Agostinelli, "Geant4—a simulation toolkit," *Nuclear Instruments and Methods in Physics Research Section A*, vol. 506, pp. 250–303, 2003.

[23] L. Sihver, D. Mancusi, K. Niita et al., "Benchmarking of calculated projectile fragmentation cross-sections using the 3-D, MC codes PHITS, FLUKA, HETC-HEDS, MCNPX_HI, and NUCFRG2," *Acta Astronautica*, vol. 63, no. 7–10, pp. 865–877, 2008.

[24] ICRP Publication 74, *Conversion Coefficients for Use in Radiological Protection Against External Radiation*, International

Commission on Radiological Protection, Stockholm, Sweden, 1996.

[25] M. Pelliccioni, "Overview of fluence-to-effective dose and fluence-to-ambient dose equivalent conversion coefficients for high energy radiation calculated using the FLUKA code," *Radiation Protection Dosimetry*, vol. 88, no. 4, pp. 279–297, 2000.